

Article

Three-Dimensional Analysis of Root Anatomy and Root Canal Curvature in Mandibular Incisors Using Micro-Computed Tomography with Novel Software

JongKi Lee ^{1,†}, Shin-Hoon Lee ^{2,†}, Jong-Rak Hong ³, Kee-Yeon Kum ⁴, Soram Oh ⁵,
Adel Saeed Al-Ghamdi ⁶, Fawzi Ali Al-Ghamdi ⁷, Ayman Omar Mandorah ⁸, Ji-Hyun Jang ^{5,9} and
Seok Woo Chang ^{5,9,*}

¹ Private Practice, Changwon 51495, Korea; dr.jongki@gmail.com

² Eunpyeong Appletree Dental Clinic, 19, Jingwan 2-ro, Eunpyeong-gu, Seoul 03306, Korea; calvin1210@hanmail.net

³ Department of Oral and Maxillofacial Surgery, Gaon Dental Hospital, 129, Dongseo-daero, Seobuk-gu, Cheonan-si, Choongcheongnam-do 31109, Korea; hongjr@skku.edu

⁴ Department of Conservative Dentistry, Dental Research Institute, National Dental Care Centre for Persons with Special Needs, Seoul National University Dental Hospital, Seoul National University School of Dentistry, Seoul 03080, Korea; kum6139@snu.ac.kr

⁵ Department of Conservative Dentistry, Kyung Hee University Dental Hospital, 23 Kyungheedaero, Dongdaemun-gu, Seoul 02447, Korea; soram0123@gmail.com (S.O.); jangjihyun@khu.ac.kr (J.-H.J.)

⁶ King Abdulaziz Hospital, Jeddah 22421, Saudi Arabia; adell1289@hotmail.com

⁷ Director of Dental Services, Ministry of Health, P.O.Box 109196, Jeddah 21351, Saudi Arabia; Fawzi2003@yahoo.com

⁸ Department of Endodontics, Restorative and Dental Materials, Faculty of Dentistry, Taif University, Taif 26571, Saudi Arabia; amandorah@tudent.edu.sa

⁹ Department of Conservative Dentistry, Kyung Hee University School of Dentistry, 23 Kyungheedaero, Dongdaemun-gu, Seoul 02447, Korea

* Correspondence: swc2007smc@khu.ac.kr

† Contributed equally to this study as first authors.

Received: 22 May 2020; Accepted: 24 June 2020; Published: 26 June 2020



Abstract: Root canal treatment of mandibular incisor is difficult because of the narrow pulp space and apical curvature. The aim of this study was to measure the anatomical indicators of the mandibular incisors in Koreans using micro-computed tomography (MCT) with novel software (Kappa 2). The MCT-scanned data from 27 mandibular incisors were reconstructed and analyzed. For each canal, 3-dimensional (3D) surface models were re-sliced at 0.1 mm intervals perpendicular to the central axis of the root canal. Root canal width, dentine thickness, and direction and degree of root canal curvatures were measured automatically on each slice. Measurements were analyzed statistically with Bhapkar test, Friedman test, and Wilcoxon signed rank test. Labial and lingual dentine thicknesses were significantly larger than mesial and distal thicknesses ($p < 0.001$). The thinnest dentine was mainly located on the mesio-lingual side of the canals in the apical third. The mean narrowest and widest canal width in the apical sixth were 0.22 mm and 0.40 mm, respectively. The canal curvature abruptly increased in the apical 0.5-mm portion. MCT with novel software provided useful anatomical information for root canal instrumentation.

Keywords: apical curvature; canal width; dentin thickness; mandibular incisor; micro-computed tomography

1. Introduction

For successful endodontic treatment, an understanding of the complex root canal anatomy as well as surrounding root dentine architecture is essential. Although the mandibular incisors usually have a single canal (72% (Leoni et al., 2014) [1], 91.1% and 82.5% (Liu et al., 2014) [2]), they pose the greatest difficulty in access preparation owing to the narrowness of the crown and pulp space in the mesio-distal direction [3]. Furthermore, mandibular incisors often have mesial and distal curves in their apical third [3], which makes the root canal preparation in this area even more difficult.

In terms of root canal preparation, the root canal width, dentin thickness around the root canal, and 3-dimensional (3D) direction and degree of the root canal curvature are relevant. However, previous studies on the root canal anatomy of the mandibular incisors were mainly focused on the root canal type, the number of root canals, and the shape of root canals [1,2]. These factors provide valuable information on the root canal anatomy itself. However, more clinically relevant information for root canal preparation is the narrowest and the widest root canal width, the dentin thickness, and the direction and degree of the root canal curvature. There have been no previous studies investigating the 3D direction or degree of root canal curvature of human mandibular incisors.

Micro-computed tomography (MCT) with mathematical modeling is an accurate and non-destructive tool for studying root canal anatomy [4]; it provides detailed information on root canal dimensions, dentin thickness, and direction and degree of the root canal curvature. Additionally, image analysis software is essential to analyze the information obtained via MCT. Our previous studies used custom-made Kappa 2 software, which produced detailed 3D measurements of various aspects of canal anatomic parameters [5–7]. This method used slices of images perpendicular to the central axis of the root canal (Figure 1A), not the long axis of the tooth, which can reduce distortions of measurements in areas where a curvature is present (Figure 1B). Our previous studies measuring the 3D root canal anatomy of the lateral incisor [8], maxillary first molar [5,9], and mandibular first molar [6] confirmed the validity of this custom-made image analyzing software (Kappa 2) in coordination with MCT.

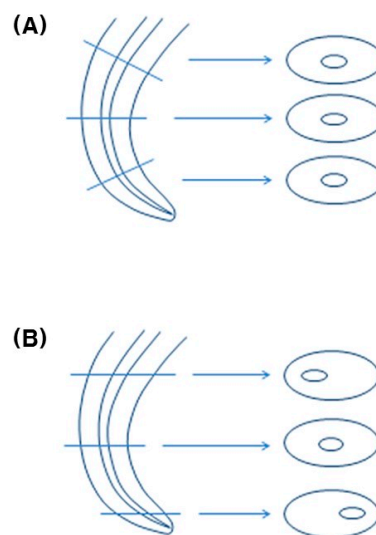


Figure 1. Slice of reconstructed image. (A) When sliced perpendicular to the long axis of the root canal, no distortions are produced. (B) When sliced perpendicular to the long axis of the tooth, distortions are produced in the images of the root canal and surrounding dentin.

The aim of this study was to determine the minimum and maximum root canal widths, dentin thickness, and 3D direction and degree of the root canal curvature in extracted human mandibular incisors.

2. Materials and Methods

This study was approved by the institutional review board of Samsung Medical Center, Seoul, Korea (SMC 2014-08-088). One-canal human mandibular incisors ($n = 27$) with mature apices and intact crowns without caries or previous root canal treatment were collected. To get rid of the calculus and adhering soft tissues, the root surfaces of collected teeth were cleaned. They were stored (4 °C) in 0.5% sodium azide solution and scanned using MCT (SkyScan 1172; Bruker-microCT, Kontich, Belgium) to acquire detailed images (voxel size = 31.8 μm^3).

2.1. Image Analysis

Images were analyzed as previously described [5–7]: 5–15 image slices that spanned each canal were selected (Figure 2). The canal width, dentin thickness, and canal curvatures were measured on re-sliced planes perpendicular to the central axis of the canal.

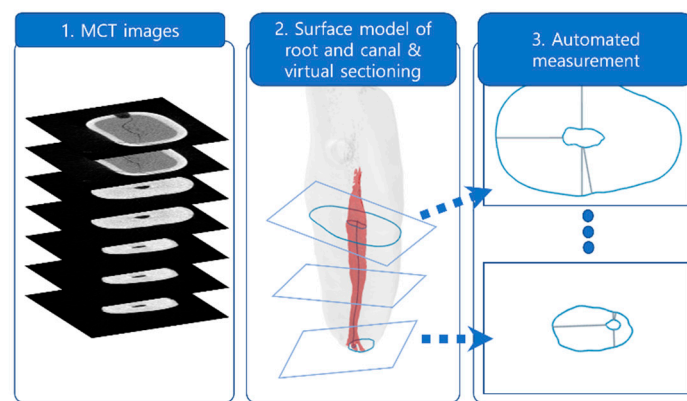


Figure 2. Overall process of the automatic measurement of root and canal dimensions. From the MCT images of mandibular incisors, 3D surface models of root canals were constructed and the central axis was plotted using V works 4.0; Cybermed, Seoul, Korea. Subsequently, surface models were sectioned perpendicular to the canal axis (at 0.1 mm intervals). Pre-defined anatomic parameters were computed in each section.

The central axes of the canals were plotted and visualized (Figure 3①). The cross-sectional plane that is perpendicular to the central axis was visualized. The canal (Figure 3②) and root (Figure 3③) outlines were marked as shown. The shortest distance between these outlines, referred to as the dentin thickness, was measured in the mesial, distal, labial, and lingual directions (Figure 3④⑤⑥⑦). The thinnest dentin thickness and direction (Figure 3⑧) were obtained in the cutting plane as mesiolabial, mesiolingual, distolabial, or distolingual. The narrowest (minimum) and widest (maximum) canal widths were measured.

To measure the curvature of the root canal, the axis of the canal was equally divided into three parts (S1, apical third; S2, middle third; and S3, coronal third). Subsequently, S1, S2, and S3 were further equally divided into apical and coronal sections, denoted as S1A, S1C, S2A, S2C, S3A, and S3C, respectively (Figure 4).

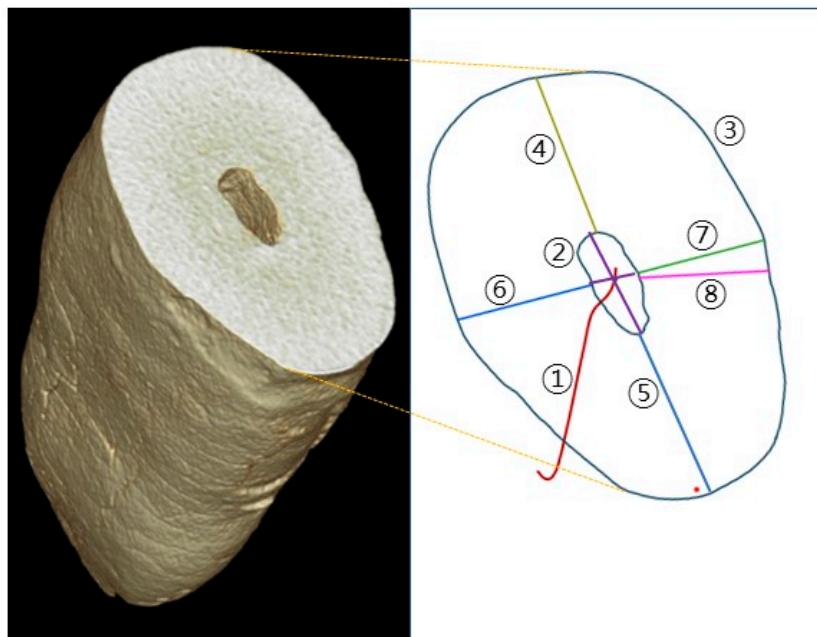


Figure 3. Graphical visualization of the measurements. Left image is the representative 3D root model, and the right image is its section; ① the central axis (red curve) of the canal; ② the root canal; ③ root outline; ④ labial dentin thickness; ⑤ lingual dentin thickness; ⑥ mesial dentin thickness; ⑦ distal dentin thickness; ⑧ the thinnest dentin thickness and its direction.

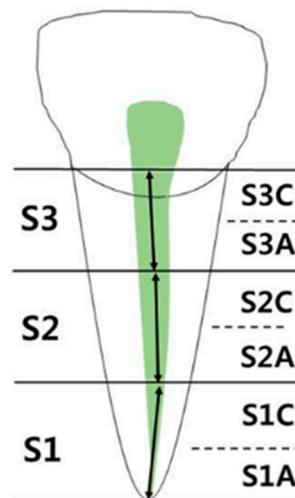


Figure 4. Axial level of the root canal

2.2. Statistical Analysis

Differences in the dentin thickness and canal curvature among directions (mesial, distal, labial, and lingual) or levels (S1A–S3C) were examined with Bhapkar’s test. The minimum dentin thickness, minimum and maximum canal widths, and canal curvature differences between six sections (S1A–S3C) were analyzed with the Friedman and Wilcoxon signed rank test ($\alpha = 0.05$).

3. Results

3.1. Dentin Thickness

The mean length of the root canals between the apex and the cementoenamel junction (CEJ) was 11.40 ± 0.96 mm. The dentin thickness gradually decreased from S3C to S1A in all mesial and distal

directions ($p < 0.05$). The mean (SD) thickness of the mesial dentin was 1.50 (0.19) mm in the S3C section and 0.66 (0.14) mm in the S1A section. The mean (SD) thickness of the distal dentin was 1.50 (0.16) mm in the S3C section and 0.66 (0.12) mm in the S1A section. The dentin thickness gradually decreased from S2C to S1A in labial and lingual directions ($p < 0.05$) (Figure 5). The mean (SD) thickness of the labial dentin was 2.28 (0.23) mm in the S3C section and 1.13 (0.23) mm in the S1A section. The mean (SD) thickness of the lingual dentin was 2.71 (0.23) mm in the S3C section and 1.27 (0.29) mm in the S1A section (Table 1). The dentin thickness was greater on labial and lingual sides compared to mesial and distal sides in all six sections (S1A–S3C) ($p < 0.001$) (Table 1, Figure 6). The mesial and distal thicknesses had no statistically significant difference in any of the six sections.

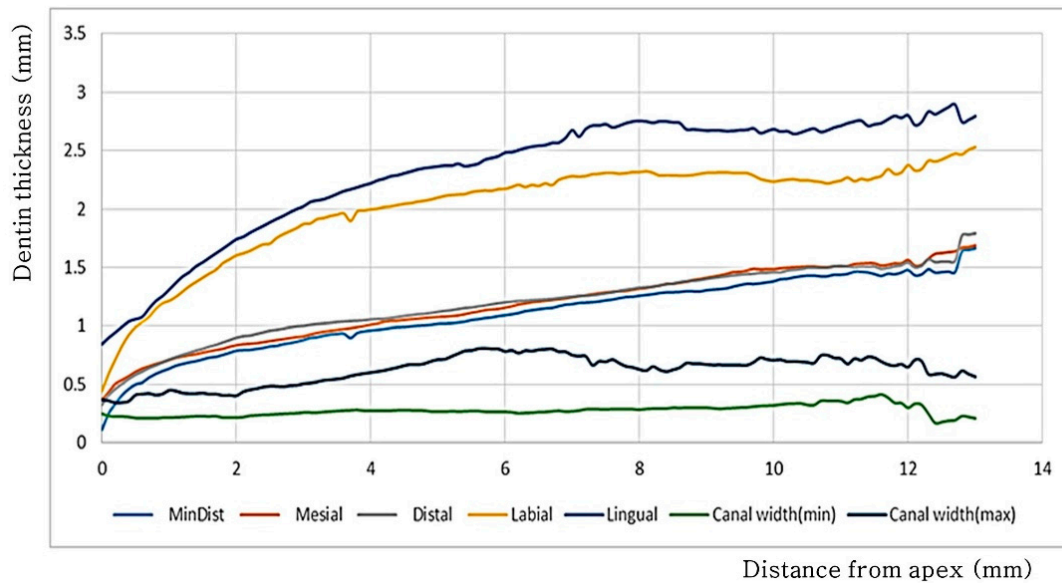


Figure 5. Measurements of dentin thicknesses. The average dentin thickness was measured on the mesial, distal, labial, and lingual sides, and the thinnest dentin thickness (MinDist), narrowest canal width (Canal width (min)), and the widest canal width (Canal width (max)) were plotted along the entire length of the canals.

Table 1. Mean values of dentin thicknesses, canal widths, and canal curvatures.

	S1A	S1C	S2A	S2C	S3A	S3C
Thinnest dentin thickness (mm)	0.56 ± 0.12	0.86 ± 0.13	1.00 ± 0.15	1.14 ± 0.14	1.30 ± 0.15	1.41 ± 0.21
Mesial dentin thickness (mm)	0.66 ± 0.14	0.91 ± 0.14	1.07 ± 0.17	1.20 ± 0.16	1.37 ± 0.16	1.50 ± 0.19
Distal dentin thickness (mm)	0.66 ± 0.12	0.98 ± 0.14	1.11 ± 0.13	1.23 ± 0.13	1.36 ± 0.13	1.50 ± 0.16
Labial dentin thickness (mm)	1.13 ± 0.23	1.81 ± 0.22	2.06 ± 0.23	2.22 ± 0.24	2.29 ± 0.23	2.28 ± 0.23
Lingual dentin thickness (mm)	1.27 ± 0.29	1.97 ± 0.28	2.32 ± 0.36	2.57 ± 0.44	2.68 ± 0.34	2.71 ± 0.23
Narrowest canal width(mm)	0.22 ± 0.05	0.25 ± 0.05	0.27 ± 0.08	0.28 ± 0.13	0.31 ± 0.15	0.30 ± 0.16
Widest canal width (mm)	0.40 ± 0.11	0.50 ± 0.17	0.70 ± 0.27	0.78 ± 0.36	0.70 ± 0.50	0.59 ± 0.38
Canal Curvature (mm ⁻¹)	0.50 ± 0.22	0.13 ± 0.05	0.09 ± 0.05	0.10 ± 0.07	0.11 ± 0.08	0.12 ± 0.06

(mean ± standard deviation).

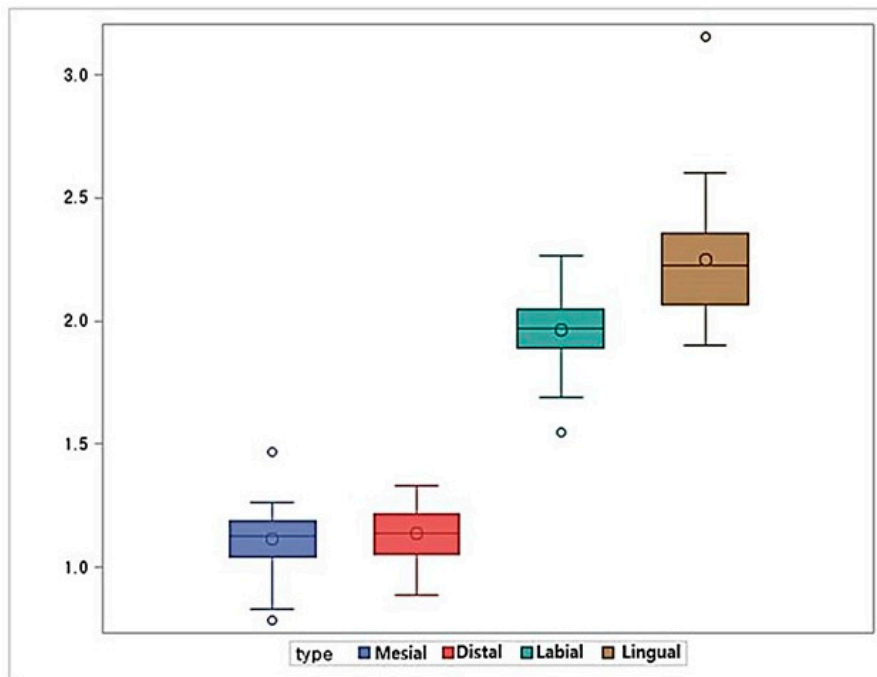


Figure 6. Average dentin thickness (mm) in mesial, distal, labial, and lingual directions.

3.2. Measurement of the Thinnest Dentin

The distance of the thinnest dentin (MinDist) gradually decreased from the CEJ towards the apex, and then decreased abruptly in the apical 0.5 mm of canals. The mean (SD) value of MinDist was 1.41 (0.21) mm at S3C section and 0.56 (0.12) mm at S1A section (Table 1, Figure 7). The direction of the MinDist was increasingly located on the mesial side. The frequencies of cross-sections in which the MinDist was located in the mesial direction were 44.45%, 51.85%, and 70.37% in the S3, S2, and S1 parts, respectively (Figure 8).

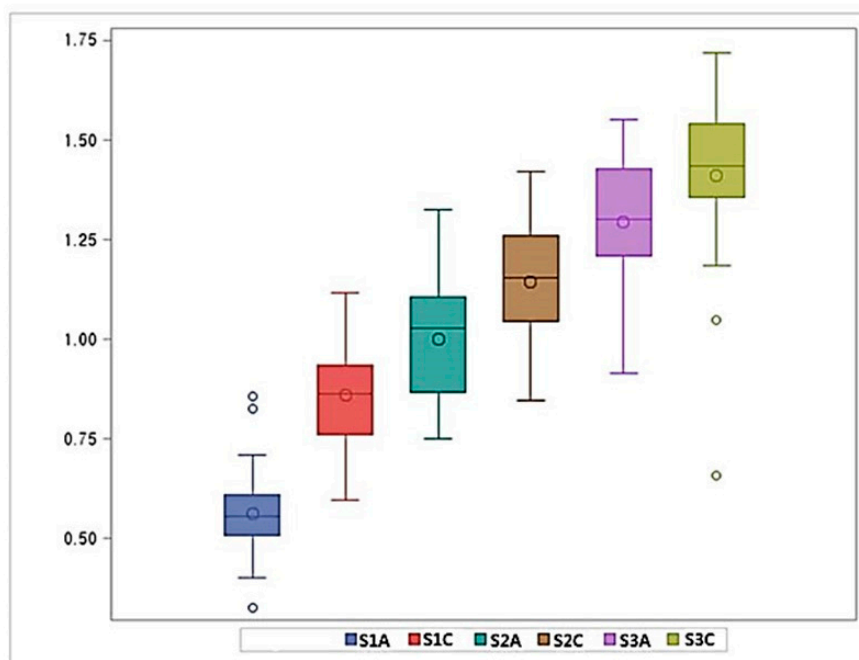


Figure 7. The thinnest dentin thickness (mm).

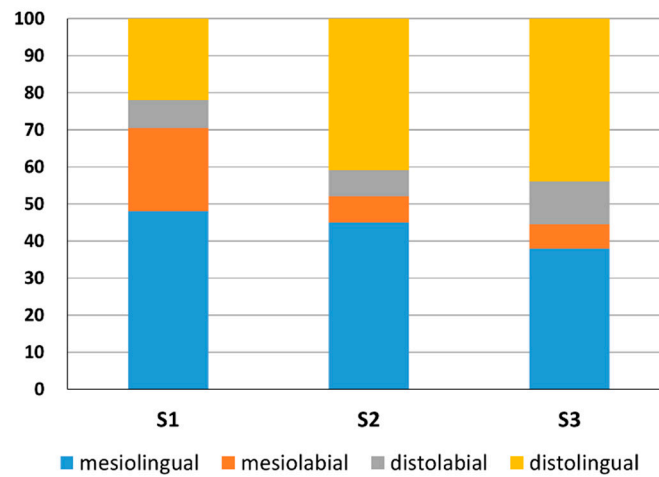


Figure 8. The relative frequency (%) of the directions with the thinnest dentin. S1: apical third; S2: middle third; S3: coronal third.

3.3. Canal Width

The mean value of the narrowest dimension of the canal width gradually decreased from S3C (0.3 mm) to S1A (0.22 mm) (Figures 5 and 9). The mean value of the widest canal width ranged from 0.4 mm (S1A) to 0.78 mm (S2C) (Figure 10, Table 1).

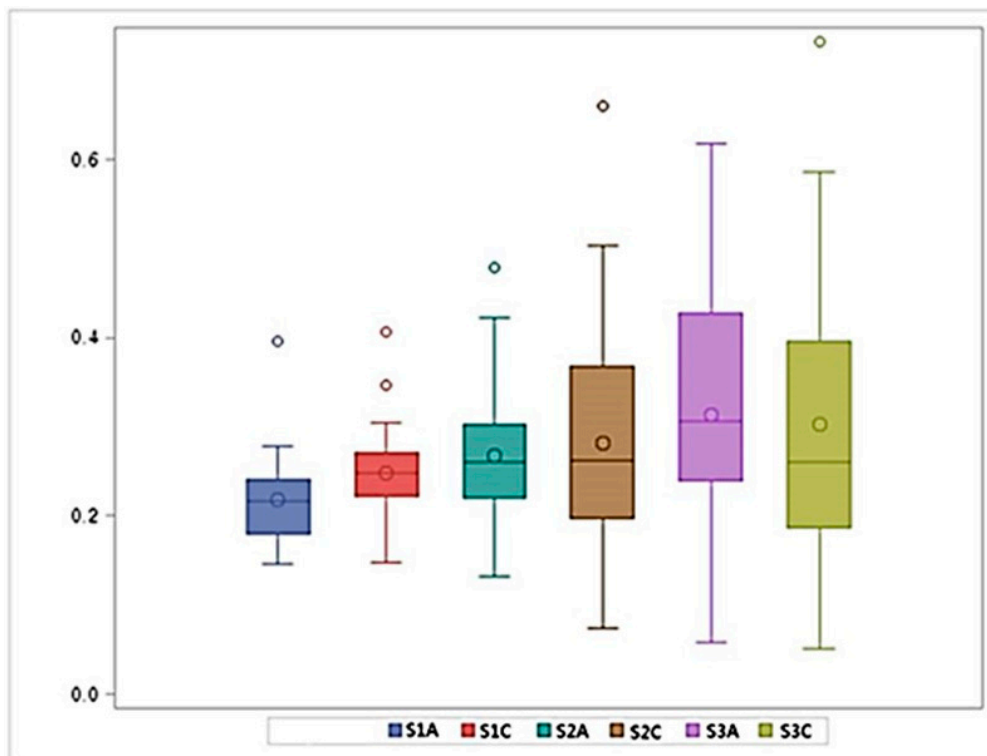


Figure 9. The narrowest canal width (mm).

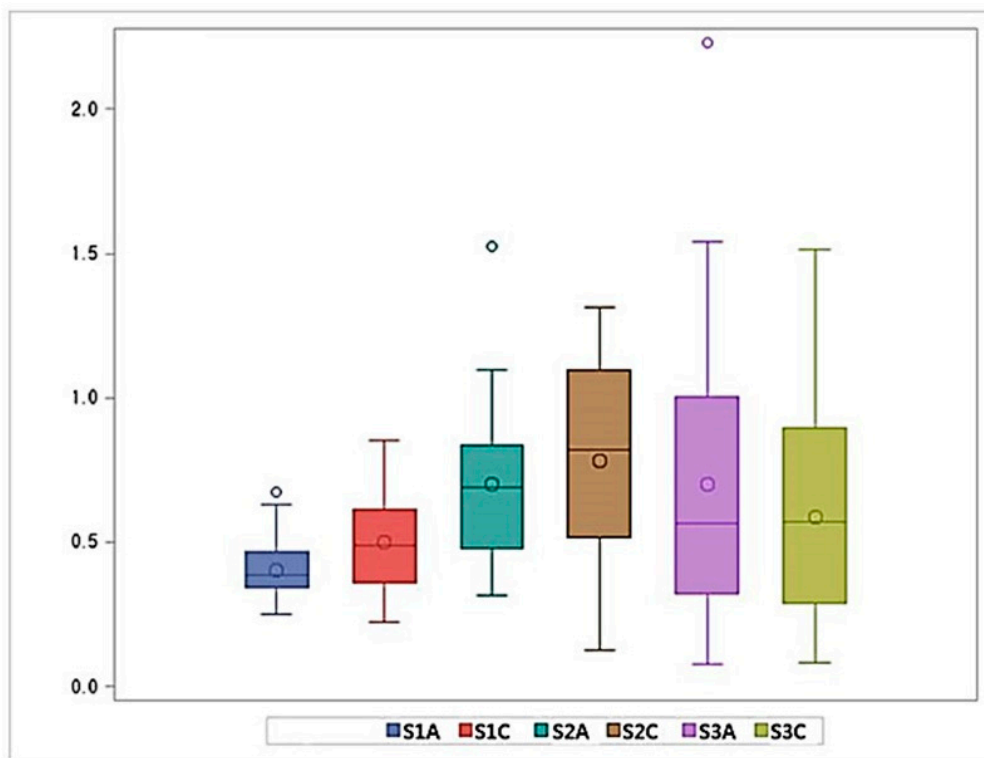


Figure 10. The widest canal width (mm).

3.4. Canal Curvature

Canal curvature increased from the S3C section ($0.12 \pm 0.06 \text{ mm}^{-1}$) to the S1C section ($0.13 \pm 0.05 \text{ mm}^{-1}$) and abruptly increased to the S1A section ($0.50 \pm 0.22 \text{ mm}^{-1}$) (Figure 11, Table 1).

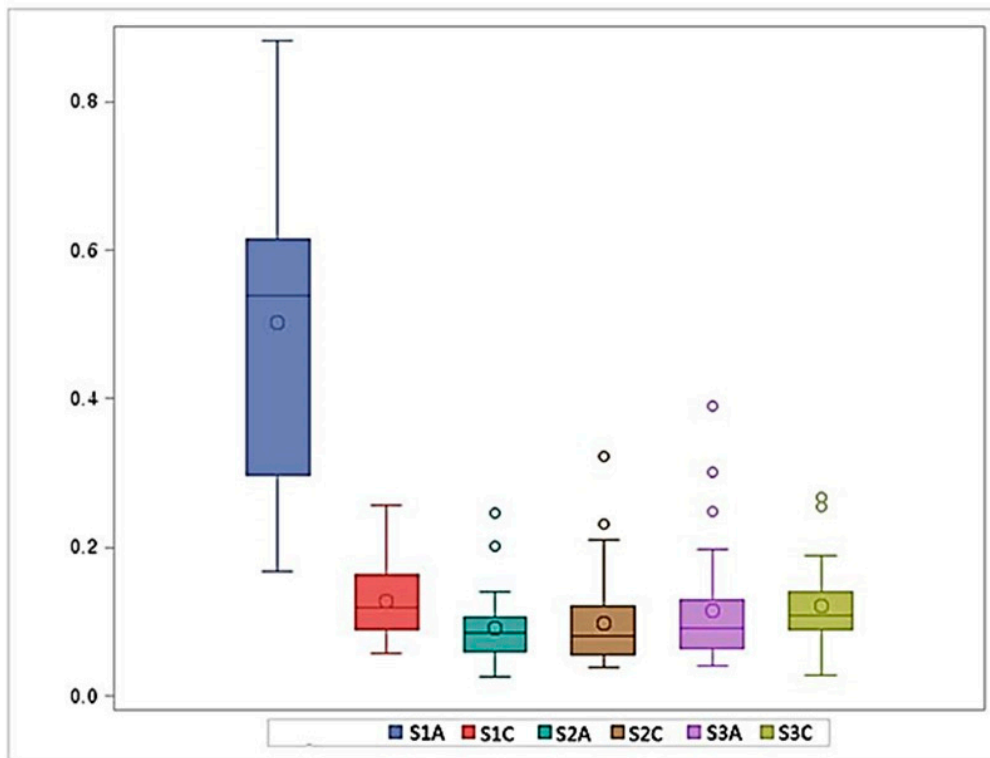


Figure 11. Average degree of canal curvatures (mm^{-1}).

4. Discussion

To avoid procedural errors in root canal preparation, information on the root canal anatomy—especially data regarding the remaining dentin thickness, narrowest and widest canal widths, and 3D direction and degree of canal curvature—is relevant. Notwithstanding the large number of root canal anatomy studies of the mandibular incisors [10–13], these variables have scarcely been measured, possibly because of the lack of customized image analyzing software. In the present study, anatomical indicators were measured using MCT combined with custom-developed software, Kappa 2, which provided 3D surface models of the roots and canals and an imaginary central axis in each cross-sectional image.

Based on our measurement results, clinicians can determine the initial apical file size when root canal treatment of mandibular incisor is performed. In the present study, the narrowest canal width was 0.22 ± 0.05 mm in the S1A section, and the widest canal width was 0.40 ± 0.11 mm in the S1A section. These results coincided with the finding reported by Milanezi de Almeida et al. that the medians of the buccolingual diameter in the apical 1 mm portion were 0.36 and 0.41 mm, respectively, in the Vertucci type I root canal and type III root canal [14]. Therefore, apical preparation should be performed at least up to the size of 0.40 mm for debridement of the necrotic pulp and removal of the infected dentin. The widest canal width of S2C (0.78 ± 0.36 mm) was greater than that of S3C (0.59 ± 0.38 mm). This interesting finding might result from root canal calcification in S3C and imply that these dentin collars should be removed for efficient root canal preparation.

Concurrently, detailed measurement of 3D canal curvature was obtained. It was the greatest in the apical region, followed by the coronal regions. The 3D canal curvature was the straightest in the mid-root region. The overall curvature of mandibular incisors measured in this study (0.18 ± 0.27 mm⁻¹) was less than that of the mesiobuccal canal of the maxillary first molar (0.22 ± 0.06 mm⁻¹) [9] and the mesiobuccal (0.26 ± 0.23 mm⁻¹) and mesiolingual canals (0.22 ± 0.18 mm⁻¹) of the mandibular first molar [7]. These results imply that root canal preparation in mandibular incisors is not as difficult as in the mesiobuccal canal of the maxillary first molar or the mesiobuccal and mesiolingual canals of the mandibular first molar.

Knowledge of the thinnest dentin, particularly in the apical part, is useful for preventing apical perforation when root canal shaping is performed. The mean (SD) value of MinDist was 0.56 (0.12) mm in the S1A section, which is susceptible to apical or strip perforation and weakening of the tooth structure. While the average mesial and distal dentin thicknesses were both 0.66 mm, the average labial and lingual dentin thicknesses were 1.13 and 1.27 mm, respectively. Therefore, instrumentation should mainly be directed toward the buccal and lingual directions, rather than the mesial and distal directions. Furthermore, the apical third (S1) has the most severe curvature, a sharp decrease in dentin thickness, and an increased frequency of the thinnest dentin being directed mesially. These features may lead to procedural errors such as transportation, ledge formation, loss of patency, and perforation. Owing to the development of the nickel-titanium rotary instruments, these iatrogenic events could be minimized by the use of flexible instruments. Previous studies reported that root canal preparation with nickel-titanium rotary files enabled the maintenance of the original canal anatomy with less canal transportation and better centering ability compared to root canal preparation with stainless-steel K files [15–17].

In the present study, detailed anatomical indicators were obtained at high precision using MCT with Kappa 2 software [18]. Nonetheless, clinical application of MCT to patients is not allowed because of the high radiation dosage and long scanning time [19,20]. A limitation of this study was the small sample size. Further studies are required in order to examine a large number of specimens.

5. Conclusions

Anatomical variables of the mandibular incisors, such as dentin thickness, direction of the thinnest dentin, root canal width, and root canal curvature, were analyzed using MCT with Kappa 2 software. The distance between the root canal wall and the root outline was the thinnest on the mesiolingual side

in the apical third. The canal width decreased gradually from the CEJ to the apex, and the root canal curvature was most severe in the apical third. Based on these measurements, clinicians can perform successful root canal preparation from a biologic perspective, without any procedural error.

Author Contributions: Conceptualization: J.L. and S.W.C.; Methodology: S-H.L., J.-R.H., and S.W.C.; Software: J.L., J.-R.H., K.-Y.K., and J.-H.J.; Validation: K.-Y.K., S.O., A.S.A.-G., and A.O.M.; Formal Analysis: J.L., S.O., A.S.A.-G., F.A.A.-G., and A.O.M.; Resources: J.-R.H. and A.S.A.-G.; Writing—Original Draft Preparation: J.L. and S.-H.L.; Writing—Review and Editing: S.O., SW.C., and K.-Y.K.; Visualization: A.S.A.-G. F.A.A.-G. A.O.M., and J.-H.J.; Supervision: S.W.C. and K.-Y.K.; Project Administration: J.L. and S.-H.L. All authors have read and agreed to the published version of the manuscript.

Funding: This research received no external funding.

Conflicts of Interest: The authors have no conflict of interest.

References

1. Leoni, G.B.; Versiani, M.A.; Pecora, J.D.; Damiao de Sousa-Neto, M. Micro-computed tomographic analysis of the root canal morphology of mandibular incisors. *J. Endod.* **2014**, *40*, 710–716. [[CrossRef](#)] [[PubMed](#)]
2. Liu, J.; Luo, J.; Dou, L.; Yang, D. CBCT study of root and canal morphology of permanent mandibular incisors in a Chinese population. *Acta Odontol. Scand.* **2014**, *72*, 26–30. [[CrossRef](#)] [[PubMed](#)]
3. Hargreaves, K.; Cohen, S. *Pathways of the Pulp*, 10th ed.; Mosby: Maryland Heights, MO, USA, 2011.
4. Chang, S.W.; Lee, J.K.; Lee, Y.; Kum, K.Y. In-depth morphological study of mesiobuccal root canal systems in maxillary first molars: Review. *Restor. Dent. Endod.* **2013**, *38*, 2–10. [[CrossRef](#)] [[PubMed](#)]
5. Lee, J.K.; Ha, B.H.; Choi, J.H.; Heo, S.M.; Perinpanayagam, H. Quantitative three-dimensional analysis of root canal curvature in maxillary first molars using micro-computed tomography. *J. Endod.* **2006**, *32*, 941–945. [[CrossRef](#)] [[PubMed](#)]
6. Kim, Y.; Perinpanayagam, H.; Lee, J.K.; Yoo, Y.J.; Oh, S.; Gu, Y.; Lee, S.P.; Chang, S.W.; Lee, W.; Baek, S.H.; et al. Comparison of mandibular first molar mesial root canal morphology using micro-computed tomography and clearing technique. *Acta Odontol. Scand.* **2015**, *73*, 427–432. [[CrossRef](#)] [[PubMed](#)]
7. Lee, J.K.; Yoo, Y.J.; Perinpanayagam, H.; Ha, B.H.; Lim, S.M.; Oh, S.R.; Gu, Y.; Chang, S.W.; Zhu, Q.; Kum, K.Y. Three-dimensional modelling and concurrent measurements of root anatomy in mandibular first molar mesial roots using micro-computed tomography. *Int. Endod. J.* **2015**, *48*, 380–389. [[CrossRef](#)] [[PubMed](#)]
8. Park, P.S.; Kim, K.D.; Perinpanayagam, H.; Lee, J.K.; Chang, S.W.; Chung, S.H.; Kaufman, B.; Zhu, Q.; Safavi, K.E.; Kum, K.Y. Three-dimensional analysis of root canal curvature and direction of maxillary lateral incisors by using cone-beam computed tomography. *J. Endod.* **2013**, *39*, 1124–1129. [[CrossRef](#)] [[PubMed](#)]
9. Park, J.W.; Lee, J.K.; Ha, B.H.; Choi, J.H.; Perinpanayagam, H. Three-dimensional analysis of maxillary first molar mesiobuccal root canal configuration and curvature using micro-computed tomography. *Oral Surg. Oral Med. Oral Pathol. Oral Radiol. Endod.* **2009**, *108*, 437–442. [[CrossRef](#)] [[PubMed](#)]
10. Pineda, F.; Kuttler, Y. Mesiodistal and buccolingual roentgenographic investigation of 7,275 root canals. *Oral Surg. Oral Med. Oral Pathol.* **1972**, *33*, 101–110. [[CrossRef](#)]
11. Madeira, M.C.; Hetem, S. Incidence of bifurcations in mandibular incisors. *Oral Surg. Oral Med. Oral Pathol.* **1973**, *36*, 589–591. [[CrossRef](#)]
12. Vertucci, F.J. Root canal anatomy of the human permanent teeth. *Oral Surg. Oral Med. Oral Pathol.* **1984**, *58*, 589–599. [[CrossRef](#)]
13. Caliskan, M.K.; Pehlivan, Y.; Sepetcioglu, F.; Turkun, M.; Tuncer, S.S. Root canal morphology of human permanent teeth in a Turkish population. *J. Endod.* **1995**, *21*, 200–204. [[CrossRef](#)]
14. Milanezi de Almeida, M.; Bernardineli, N.; Ordinola-Zapata, R.; Villas-Boas, M.H.; Amoroso-Silva, P.A.; Brandao, C.G.; Guimaraes, B.M.; Gomes de Moraes, I.; Hungaro-Duarte, M.A. Micro-computed tomography analysis of the root canal anatomy and prevalence of oval canals in mandibular incisors. *J. Endod.* **2013**, *39*, 1529–1533. [[CrossRef](#)] [[PubMed](#)]
15. Tasdemir, T.; Aydemir, H.; Inan, U.; Unal, O. Canal preparation with Hero 642 rotary Ni-Ti instruments compared with stainless steel hand K-file assessed using computed tomography. *Int. Endod. J.* **2005**, *38*, 402–408. [[CrossRef](#)] [[PubMed](#)]
16. Moore, J.; Fitz-Walter, P.; Parashos, P. A micro-computed tomographic evaluation of apical root canal preparation using three instrumentation techniques. *Int. Endod. J.* **2009**, *42*, 1057–1064. [[CrossRef](#)] [[PubMed](#)]

17. Gergi, R.; Rjeily, J.A.; Sader, J.; Naaman, A. Comparison of canal transportation and centering ability of twisted files, Pathfile-ProTaper system, and stainless steel hand K-files by using computed tomography. *J. Endod.* **2010**, *36*, 904–907. [[CrossRef](#)] [[PubMed](#)]
18. Paque, F.; Zehnder, M.; De-Deus, G. Microtomography-based comparison of reciprocating single-file F2 ProTaper technique versus rotary full sequence. *J. Endod.* **2011**, *37*, 1394–1397. [[CrossRef](#)] [[PubMed](#)]
19. Rhodes, J.S.; Ford, T.R.; Lynch, J.A.; Liepins, P.J.; Curtis, R.V. Micro-computed tomography: A new tool for experimental endodontology. *Int. Endod. J.* **1999**, *32*, 165–170. [[CrossRef](#)] [[PubMed](#)]
20. Gu, Y.; Lee, J.K.; Spangberg, L.S.; Lee, Y.; Park, C.M.; Seo, D.G.; Chang, S.W.; Hur, M.S.; Hong, S.T.; Kum, K.Y. Minimum-intensity projection for in-depth morphology study of mesiobuccal root. *Oral Surg. Oral Med. Oral Pathol. Oral Radiol. Endod.* **2011**, *112*, 671–677. [[CrossRef](#)] [[PubMed](#)]



© 2020 by the authors. Licensee MDPI, Basel, Switzerland. This article is an open access article distributed under the terms and conditions of the Creative Commons Attribution (CC BY) license (<http://creativecommons.org/licenses/by/4.0/>).